



## Late Pleistocene dust deposition in the Patagonian steppe - extending and refining the paleoenvironmental and tephrochronological record from Laguna Potrok Aike back to 55 ka

Torsten Haberzettl<sup>a,b,\*</sup>, Flavio S. Anselmetti<sup>c</sup>, Sabine W. Bowen<sup>d</sup>, Michael Fey<sup>e</sup>, Christoph Mayr<sup>f</sup>, Bernd Zolitschka<sup>e</sup>, Daniel Ariztegui<sup>g</sup>, Barbara Mauz<sup>h</sup>, Christian Ohlendörfer<sup>e</sup>, Stephanie Kastner<sup>e</sup>, Andreas Lücke<sup>i</sup>, Frank Schäbitz<sup>j</sup>, Michael Wille<sup>j</sup>

<sup>a</sup> Institut des sciences de la mer de Rimouski (ISMER), University of Québec at Rimouski (UQAR), 310, allée des Ursulines, Rimouski, Québec, G5L 3A1, Canada

<sup>b</sup> GEOTOP Research Centre, P.O. Box 8888, Succ. Centre-ville, Montréal, Québec, H3C 3P8, Canada

<sup>c</sup> Eawag, Swiss Federal Institute of Aquatic Science and Technology, Department of Surface Waters, Überlandstr. 133, 8600 Dübendorf, Switzerland

<sup>d</sup> Institute for Geophysics, Jackson School of Geosciences, The University of Texas at Austin, 10100 Burnet Rd., Austin, TX 78758, USA

<sup>e</sup> Geomorphology and Polar Research (GEOPOLAR), Institute of Geography, University of Bremen, Celsiusstr. FVG-M, 28359 Bremen, Germany

<sup>f</sup> GeoBio-Center and Department of Earth and Environmental Sciences, University of Munich, Richard-Wagner-Str. 10, 80333 Munich, Germany

<sup>g</sup> Section of Earth & Environmental Sciences, University of Geneva, Rue de Maraîchers 13, 1205 Geneva, Switzerland

<sup>h</sup> Department of Geography, University of Liverpool, Liverpool L69 7ZT, UK

<sup>i</sup> Institute for Chemistry and Dynamics of the Geosphere (ICG) V: Sedimentary Systems, Research Center Jülich, 52425 Jülich, Germany

<sup>j</sup> Seminar for Geography and Education, University of Cologne, Gronewaldstr. 2, 50931 Cologne, Germany

### ARTICLE INFO

#### Article history:

Received 26 March 2009

Received in revised form

29 July 2009

Accepted 31 July 2009

### ABSTRACT

Paleoenvironmental records extending well into the last glacial period are scarce in the steppe regions of southern South America. Here, we present a continuous record for the past 55 ka from the maar lake Laguna Potrok Aike (51°58' S, 70°23' W, southern Patagonia, Argentina). Previous studies on a sedimentary core from a lake level terrace near the northern margin of the lake covered parts of Oxygen Isotope Stage (OIS) 3 (59–29 ka) whereas a second core from the centre of the basin comprised the last 16 ka. Tephrostratigraphical constraints and OSL ages from a third core located below the lake level terrace provide the crucial piece to close the gap between the previous coring sites. High-resolution XRF and magnetic susceptibility as well as grain size data indicate a positive hydrological balance alongside with relatively high aeolian activity during the glacial which is contemporaneous with increased dust fluxes in Antarctica. This is therefore the first evidence for contemporaneity of aeolian deposition in both the target area (Antarctica) and in the major source area of Patagonia. During the Holocene climatic conditions driving sediment deposition seem to have been more variable and less dominated by wind compared to glacial times. The identification of a minor lake level lowering at approximately 4 cal ka BP allows to refine earlier paleoenvironmental reconstructions for the Holocene. Within error margins the OSL ages are consistent with published radiocarbon-dated records offering hence a valuable tool for further studies of the sediments from Laguna Potrok Aike. The new chronology confirms the age of three tephra layers up to now only found in Laguna Potrok Aike sediments and ascribed to OIS 3.

© 2009 Elsevier Ltd. All rights reserved.

### 1. Introduction

An increasing number of terrestrial paleoclimatic records from southern South America has been published during the last decade (Gilli et al., 2001; Markgraf et al., 2003; Gilli et al., 2005a,b; Mayr et al., 2005; Villa-Martínez and Moreno, 2007; Whitlock et al., 2007;

Unkel et al., 2008). These archives mostly cover the Lateglacial and/or the Holocene. Hence, little is known about the Patagonian climate before the Last Glacial Maximum (Roig et al., 2001; Kaplan et al., 2008; Mancini et al., 2008). Attempts have already been made to reconstruct wind patterns in Patagonia indirectly on longer time periods using aeolian dust deposited in Antarctic ice cores, as Patagonia proved to be the main dust source for central East Antarctica during cold periods within the late Quaternary (Basile et al., 1997; Petit et al., 1999; Delmonte et al., 2004, 2008).

\* Corresponding author: Tel.: +1 418 723 1986x1664; fax: +1 418 724 1842.

E-mail address: [Torsten.Haberzettl@uqar.qc.ca](mailto:Torsten.Haberzettl@uqar.qc.ca) (T. Haberzettl).

Recently, sediment cores from the maar lake Laguna Potrok Aike in southern Patagonia ( $51^{\circ}58'S$ ,  $70^{\circ}23'W$ , Figs. 1 and 2) provided terrestrial paleoclimatic and paleoenvironmental data not only from the Lateglacial (since 16,000 cal BP) and the Holocene (Haberzettl et al., 2005, 2006; Zolitschka et al., 2006; Haberzettl et al., 2007a,b; Mayr et al., 2007b; Wille et al., 2007; Anselmetti et al., 2009; Mayr et al., 2009) but also for a hitherto temporally not precisely defined part of OIS 3 (Haberzettl et al., 2008). This sedimentary record (core 6, Fig. 2) extending back into the last glacial (OIS 3) is located in a subaquatic lake level terrace and contains a hiatus, which was identified during a high-resolution 3.5 kHz seismic survey (Anselmetti et al., 2009). Sediments above this hiatus show a continuous deposition from 6.75 cal ka BP to the present whereas the only existing age below it was provided by a  $^{14}C$  date of  $44.8 \pm 2$  ka BP (uncalibrated as beyond the southern and northern hemisphere calibration curves of CALIB 5.0.2) (Haberzettl et al., 2008). Hence, it was impossible to set up a chronology below the hiatus in order to establish time constraints of environmental changes. In this study, we extend the continuous and high-resolution 16 ka paleoenvironmental record from the centre of Laguna Potrok Aike (core 12 in Fig. 2) (Haberzettl et al., 2007a) back in time to 55 ka. We combine the discontinuous littoral record of core 6 with the new littoral core 5 continuously and conformably spanning the time interval across this hiatus.

Furthermore, we present the first optically stimulated luminescence (OSL) ages for this combined littoral record and for the 16 ka spanning profundal sediment core 12 assessing the applicability of optical dating to sediments from Laguna Potrok Aike. The latter will potentially provide a reliable chronology beyond the limit of radiocarbon dating of sediments from Laguna Potrok Aike recovered during the ICDP (International Continental Scientific Drilling Program) deep drilling project PASADO (Potrok Aike maar lake Sediment Archive Drilling project).

## 2. Regional setting

The circular maar lake Laguna Potrok Aike is located in southern Santa Cruz (Patagonia, Argentina), 85 km west of the city of Río

Gallegos and  $\sim 80$  km north of the Strait of Magellan. It is situated in the western part of the Pali Aike Volcanic Field (Fig. 1). With a maximum W–E-extension of about 150 km and a maximum N–S-extension of ca 50 km this tectonovolcanic belt has an area of  $\sim 4500$  km $^2$  (Mazzarini and D’Orazio, 2003). Petrologically, it consists of alkali-olivine basalts with an age range from 3.8 Ma in the western part to 0.01 Ma in the east (Corbella, 2002). The detailed geological and volcanological development of these back arc Patagonian plateau lavas has been discussed before (Skewes, 1978; D’Orazio et al., 2000; Corbella, 2002; Mazzarini and D’Orazio, 2003).

Laguna Potrok Aike itself was created by an explosive eruption caused by the contact of rising magma with groundwater. Its formation is Ar/Ar-dated from the phreatomagmatic tephra on glass fragments as  $0.77 \pm 0.24$  Ma (Zolitschka et al., 2006). The immediate surrounding of Laguna Potrok Aike is formed by Pleistocene basal till exceeding this age. However, since the late Pleistocene the studied area was not glaciated as the so called Llanquihue Glaciation, equivalent to the Weichselian or Wisconsin (Rabassa and Clapperton, 1990), did not reach the Pali Aike Volcanic Field (Zolitschka et al., 2006).

In 2003 the lake level of Laguna Potrok Aike was at 113 m asl. At that point the lake had a maximum water depth of 100 m and a diameter of 3.5 km (Fig. 2). Recent observations indicate that annual lake level fluctuations are less than 1 m. However, the lake level has been rising by more than 1 m since March 2003 (Haberzettl et al., 2007a). Although the morphological catchment area of the lake exceeds 200 km $^2$  reaching far south into the Chilean part of the Pali Aike Volcanic Field, model calculations imply that the modern high evaporation/precipitation ratio (E/P) of up to 24 (Haberzettl et al., 2005) is responsible that ca 60% of the runoff to Laguna Potrok Aike undergoes evaporation (Mayr et al., 2007a). These high evaporation rates originate from the high wind speeds from predominantly westerly directions reaching average monthly speeds of up to  $9$  m s $^{-1}$  during early summer (Endlicher, 1993). Owing to the strong winds that enforce polymictic conditions today, there is almost no stratification of the waterbody in summer and freezing in winter is inhibited (Zolitschka et al., 2006). In combination with the rain shadow effect of the Andes the high wind speeds cause a precipitation decrease

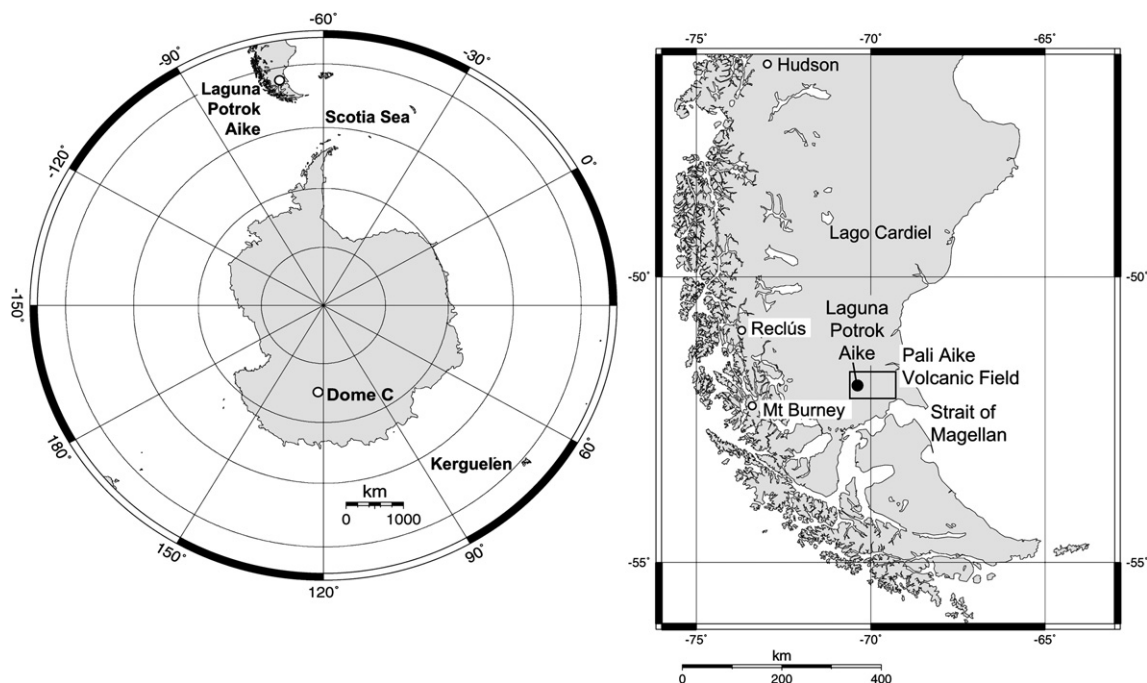
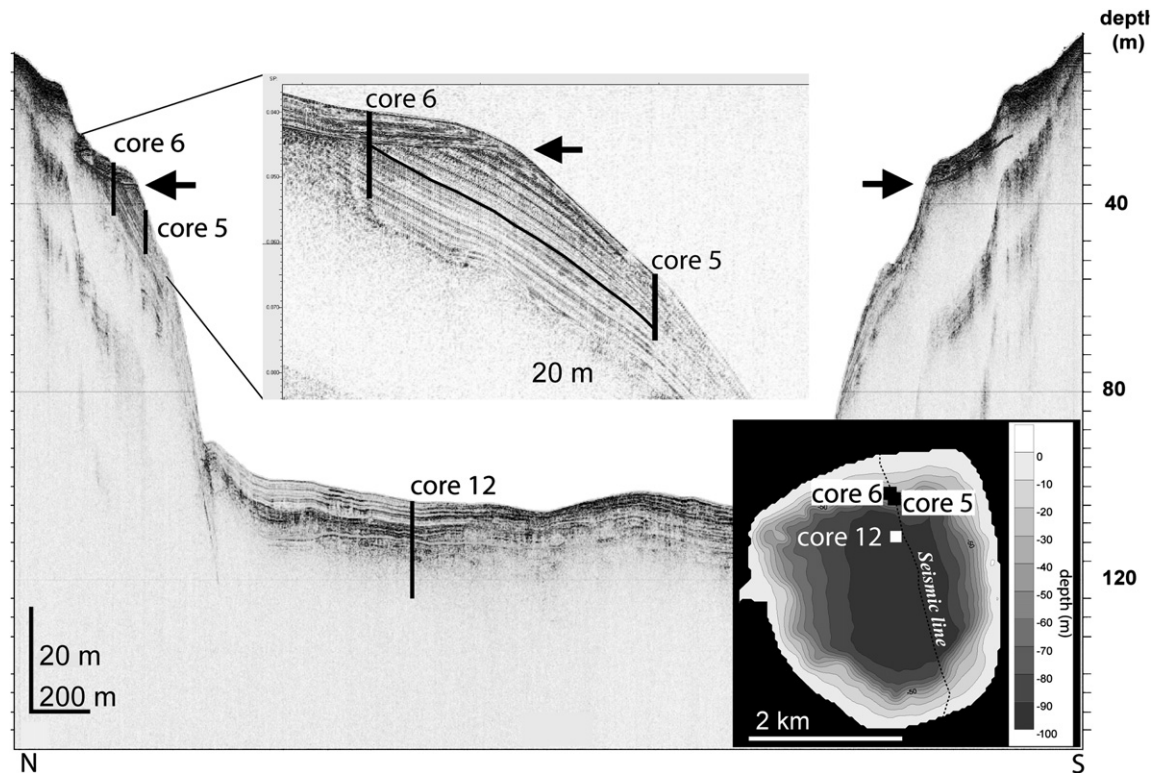


Fig. 1. Location of Laguna Potrok Aike and other sites discussed in the text.



**Fig. 2.** Seismic profiles of Laguna Potrok Aike. Drilling sites of sediment cores 5, 6 and 12 are shown. Black line of the magnified seismic section (inset in the center) indicates the correlation marker layer (older Reclús tephra) combining the records of core 5 and core 6. Arrows indicate location of the hiatus related to core 6. The inset on the right bottom area shows the bathymetry including positions of drilling sites as well as the seismic line.

from west to east resulting in semiarid conditions with less than 300 mm annual precipitation in the area. Precipitation is almost equally distributed around the wind rose, with maxima from southwestern and northern directions (Haberzettl, 2006). However, compared to the frequency of wind directions, more precipitation is brought in with air masses of easterly origin than from other directions. Thus, a relatively moderate increase in the occurrence of easterly wind directions results in a considerable increase of precipitation (Mayr et al., 2007b).

In the past Laguna Potrok Aike experienced distinct lake level variations with a pronounced recession during the Mid-Holocene climate optimum (Haberzettl et al., 2008; Anselmetti et al., 2009) and a high lake level during the northern hemisphere Little Ice Age chronozone (Haberzettl et al., 2005). As a result of these ancient lake level fluctuations numerous well-preserved subaerial as well as subaquatic lake level terraces have developed around the lake covered with different vegetation above the present shore line. Laguna Potrok Aike belongs to the few permanent lakes in the dry lands of southern Patagonia which assures a continuous sediment record even during dry periods (Haberzettl et al., 2005). Today, Laguna Potrok Aike is a terminal lake. However, there is geomorphological evidence for an overflow 21 m above the present (2003) lake level. The exact timing of this overflow is still unknown but paleoclimatic interpretations indicate that an overflowing regime existed before 13.1 ka (Haberzettl et al., 2007a).

### 3. Material and methods

#### 3.1. Field methods

A ~70 km-long grid of high-resolution single-channel seismic data was acquired in February 2003 using a 3.5 kHz pinger system

with a vertical resolution of ~10 cm (Fig. 2). The survey was performed with the steel-hulled catamaran RV “Lago Cardiel” and GPS-based navigation. Seismic data were stored digitally in SEG-Y format allowing further processing and interpretation. A 2–6.5 kHz band-pass filter was applied to the raw data (Anselmetti et al., 2009). Coring locations were selected based on this seismic survey as follows: a) three parallel cores (PTA03/12, PTA03/13 and PTA02/4) from the centre of the lake at 100 m water depth form a composite record here termed core 12 (Haberzettl et al., 2007a); b) core PTA03/6 (termed core 6) retrieved from a lake level terrace at 30 m water depth comprising an unconformity caused by a hiatus which is related to a low lake level (Haberzettl et al., 2008); and c) core PTA03/5 (core 5, this study) located in a conformable sedimentary succession at 47 m water depth i.e., below the lake level terrace (all Fig. 2). Overlapping sediment cores from these three sites were recovered using a hand-driven UWITEC piston coring system ([www.uwitec.at](http://www.uwitec.at)) with acrylic liners of 60 mm inner diameter.

#### 3.2. Non-destructive laboratory methods

In the laboratory, cores were stored in darkness at 4 °C before being split, photographed and described in detail. Non-destructive magnetic susceptibility ( $k$ ) and XRF of cores 12 and 6 were scanned in 1 cm-increments using a Bartington MS2E point sensor (Zolitschka et al., 2001) and a CORTEX (Co rescanner Texel) XRF-scanner (Jansen et al., 1998; Zolitschka et al., 2001; Richter et al., 2006).  $k$  of core 5 was scanned with 4 mm-resolution using the same type of point sensor. The XRF-scanning step size for the uppermost section of core 5 (PTA03/5-1: 87.1 cm) was 1 mm using an ITRAX core scanner (Croudace et al., 2006; St-Onge et al., 2007). For the remaining sections of the record a step size of 5 mm was applied. Ca-profiles obtained by XRF-scanning, magnetic susceptibility data and

photographs were used for correlation of overlapping core sections and for establishment of composite records. Other elements obtained by XRF-scanning were only used in critical parts. All depths correspond to these composite depth scales. The latter also applies to a combined profile of cores 5 and 6, hereafter termed profile 5 + 6.

### 3.3. Dating

#### 3.3.1. Proximal tephra from other sedimentary archives

Radiocarbon ages of proximal tephra deposits from other sedimentary archives were taken from literature (Stern, 1990; Naranjo and Stern, 1998; Kilian et al., 2003; McCulloch et al., 2005). They were calibrated using the Calib 5.0.2 software with the IntCal04 calibration curve (Stuiver and Reimer, 1993; Reimer et al., 2004) and petrologically correlated with tephra layers from cores 12 and 5.

#### 3.3.2. Radiocarbon dating

AMS  $^{14}\text{C}$  age determinations on cores 12 and 6 (stems of aquatic mosses, calcite fraction of bulk samples, twig of *Berberis*, bone of rodent, etc.) were carried out at the Poznań Radiocarbon Laboratory (Poland). The detailed methodology and results are published elsewhere (Haberzettl et al., 2007a, 2008). Unfortunately, no macrofossil remains suitable for radiocarbon dating were available in core 5. The previously uncalibrated radiocarbon age below the hiatus in core 6 (POZ-6098, Table 1, Figs. 3 and 4) was calibrated with the software CalPal (Weninger et al., 2004) because it exceeds the calibration curves of CALIB 5.0.2 (McCormac et al., 2004; Reimer et al., 2004).

#### 3.3.3. Optical dating

For optically stimulated luminescence dating (OSL), 8–20 cm long sediment sections were sampled in subdued laboratory safe light. The outer rim of the sediment was removed from the sample to avoid contamination with material that could have been exposed to light after core recovery. Analyses were performed at the Luminescence Dating Laboratory of the Department of Geography, University of Liverpool (LV). Three OSL samples (LV 125, 126, 127) were taken from core 12, two samples (LV 122, 123) from core 5 and one sample (LV 124) from core 6 (Table 2, Figs. 3–5).

The samples did not provide quartz and therefore feldspars grains of 4–15  $\mu\text{m}$  were extracted from the sediment using conventional techniques. This laboratory procedure involved removal of organic matter using hydrogen peroxide (30%), and removal of calcium carbonate using hydrochloric acid (30%). Grains were then separated by settling in cylinders following Stokes' Law, first in slightly alkaline water and then in acetone. An acetone suspension of the subsample was pipetted onto aluminium discs making up 2.5 mg aliquots. A Risø DA-15 TL/OSL reader equipped

with an EMI 9235QB photomultiplier tube and 21 LEDs providing  $\sim 30 \text{ mW cm}^{-2}$  at 870 nm was used for luminescence measurements. The OSL light was detected through a filter combination ( $2 \times \text{BG3}$ , 3 mm;  $1 \times \text{BG39}$ , 8 mm;  $1 \times \text{GG400}$ , 3 mm) providing 390–450 nm transmission.

For  $D_e$ -estimation the multiple aliquot additive dose protocol was employed. This protocol requires around 80 aliquots to determine the alpha and beta equivalent dose ( $D_{e\alpha}$ ,  $D_{e\beta}$ ), the  $a$ -value and the anomalous fading rate. All irradiated aliquots were stored at room temperature for at least 30 days before IRSL measurements. Annual dose rates were calculated from radionuclide concentrations determined using high-resolution, low-level  $\gamma$ -spectrometry and the burial depth of the sample. Gaussian error propagation at the  $1\sigma$ -level was applied including all known systematic and random errors. Further details about the method is published elsewhere (Mauz et al., 2002).

### 3.4. Tephra analyses

Distal tephra from core 12 (sections PTA03/12-12, PTA03/12-15, and PTA03/12-22, hereafter termed t12-12, t12-15, t12-22) at 1075 cm, 1320 cm, and 1861 cm sediment depth (Figs. 4 and 5), and core 6 (sections PTA03/6-4, PTA03/6-8, and PTA03/6-10, hereafter t6-4, t6-8, t6-10) at 379 cm, 643 cm, and 859 cm sediment depth (Fig. 4) have been geochemically analysed in former studies, and correlated with specific eruptive events of Mt Burney, Reclús and Hudson volcanoes (Haberzettl et al., 2007a, 2008). In core 5, four distinct tephra layers have been identified at 78 cm (section PTA03/5-1, hereafter t5-1), 96 cm, 142.5 cm (both section PTA03/5-2, hereafter t5-2a, t5-2b) and 640 cm (section PTA03/5-8, hereafter t5-8) sediment depth (Fig. 4). In order to enable a stratigraphic correlation with cores 6 and 12, the two oldest tephra layers in core 5 (t5-2b, t5-8; Fig. 4) were additionally analysed using comparable preparation techniques. Ash samples were soaked in a 10% hydrogen peroxide solution in order to remove organic matter before drying. Polished thin sections of volcanic glass shards were prepared for microprobe analyses. A JEOL-8200 instrument at the Department of Geological Sciences, The University of Texas at Austin, was used with the following measuring conditions: 15 kV voltage, 10 nA beam current, a 10  $\mu\text{m}$  beam size, and sodium analysed first. International mineral and glass standards (KN18) were applied for calibration. The data of analyses of individual tephra layers were recalculated to 100wt.% and given as a mean with  $1\sigma$  standard deviation of  $n$  glass shards. Geochemical data for the other tephra layers have been published previously (Haberzettl et al., 2007a, 2008). The two youngest tephra layers in the uppermost sections of core 5 (t5-1, t5-2a) were correlated based on their stratigraphic position in the profile (Fig. 4) and on their sedimentological-mineralogical composition

**Table 1**  
Dating results for profile 5 + 6 in stratigraphic order.

Type of date	Material	Depth in core (cm)	Age (BP)	Error	Median cal. age / OSL age (years)	Min age ( $2\sigma$ )	Max age ( $2\sigma$ )	Lab No/reference
14C Hudson tephra	Hudson tephra	78	6915 <sup>a</sup> 7635 <sup>a</sup>	40 40	8100	7670	8535	Kilian et al. 2003/ Haberzettl et al. 2007a
14C Mt Burney tephra	Mt Burney tephra	96	7635 <sup>a</sup> 7890 <sup>a</sup>	40 40	8680	8380	8975	Kilian et al. 2003/ Haberzettl et al. 2007a
OSL	feldspars	111.5			8500	7500	9500	LV 123
14C Reclús tephra	Reclús tephra	142.5	12,638 <sup>a</sup>	60	14,900	14,605	15,190	McCulloch et al. 2005/ Haberzettl et al. 2007a
OSL	feldspars	179			13,300	11,500	15,100	LV 122
radiocarbon	macrofossil	988.5	44,800	2000	48,500	45,975	51,025	POZ-6098/ Haberzettl et al. 2007a
OSL	feldspars	1165.75			53,000	47,000	59,000	LV 124

<sup>a</sup> Tephra dates from literature were (re-)calibrated with Calib 5.0.2 (Haberzettl et al. 2007a).

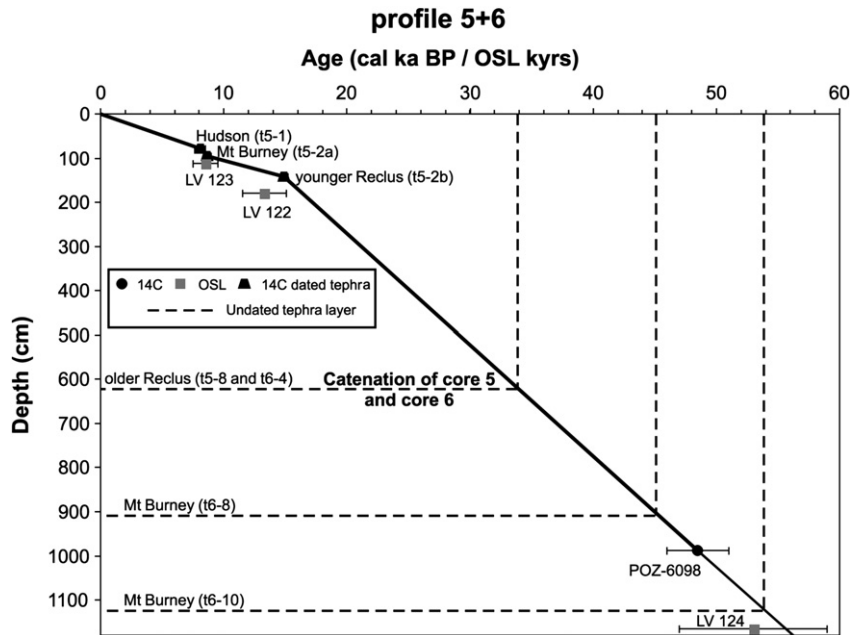


**Fig. 3.** Age-depth model of profile 5+6 indicating stratigraphic positions of tephra layers. Note that t5-8 and t6-4 are geochemically identical tephra layers (older Reclus tephra) used as marker layers for combining the two sedimentary records. OSL ages are plotted for comparison. Error bars for radiocarbon dated tephra layers are smaller than the respective symbol.

(thickness of tephra layers, grain size of tephra components and mineral-lithic assemblages).

**4. Results**

**4.1. Tephra analyses**

The tephra t5-2b located at 142.5 cm sediment depth in core 5 (Fig. 4) is a 1.5 cm-thick, beige vitric ash layer (maximum diameter: 160 μm, mean diameter: 30 μm) comprising abundant phenocrysts of clinopyroxene, orthopyroxene, zoned plagioclase and rare amphibole. Corroded quartz xenocrysts and clasts of plagioclase crystals are common. The chemical composition of micro-pumices and glass shards is heterogeneous and dominantly rhyolitic and

dacitic (Table 3). The main rhyolitic glass component is characterized by high concentrations in SiO<sub>2</sub> (76.3–77.5 wt%, normalized data), relatively low Al<sub>2</sub>O<sub>3</sub> values (12.7–14.0 wt%) and a K<sub>2</sub>O/Na<sub>2</sub>O ratio of 0.6. The dacitic glass component shows a lower silica concentration of ca 66.7 wt%, a higher content in Al<sub>2</sub>O<sub>3</sub> (ca 17.5 wt%) and a lower K<sub>2</sub>O/Na<sub>2</sub>O ratio of 0.4 (Table 3). The t5-2b tephra corresponds to a Late Pleistocene distal tephra layer from Reclus volcano and is geochemically the same as t12-22, 1885 cm (Figs. 4–6) showing an age of 14.9 cal ka BP (Haberzettl et al., 2007a).

The oldest tephra layer t5-8 in core 5 at 640 cm sediment depth (Fig. 4) is a 2.5 cm-thick, beige vitric ash (maximum diameter: 210 μm, mean diameter: 40 μm). Glass shards dominate among the tephra components revealing two different major-element chemistries: the main glass population is rhyo-dacitic in composition

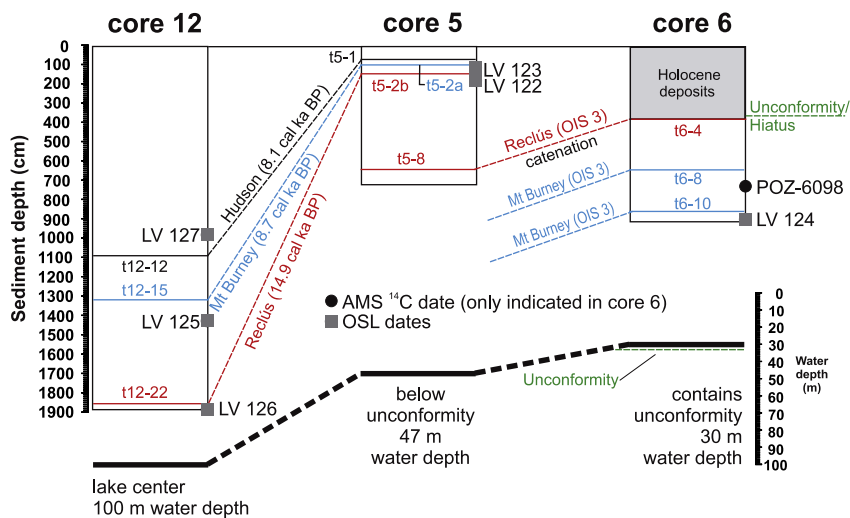


**Fig. 4.** Correlation of cores 5, 6 and 12. Also indicated are the hiatus which causes the unconformity, OSL dates, the radiocarbon date below the hiatus in core 6, and tephra layers. The older Reclus (OIS 3) tephra represents the catenation between core 5 and core 6. The line graph at the bottom shows the water depths of the recovered records and the depth of the hiatus

**Table 2**  
Analytical data used for optical age (OSL) estimates

Core number	Mean depth in respective core (cm)/Depth in composit profile (cm)	Age (years)	$\pm 1\sigma$ (years)	Mineral	Water content (%)	Grain size ( $\mu\text{m}$ )	U ( $\mu\text{g g}^{-1}$ )	Th ( $\mu\text{g g}^{-1}$ )	K (wt %)	a-value	Defective ( $\text{Gy ka}^{-1}$ )	De (Gy)	Lab No
core 5	111.5/111.5	8,500	800	feldspars	70 $\pm$ 9	4–15	1.68 $\pm$ 0.06	6.07 $\pm$ 0.16	1.38 $\pm$ 0.03	0.06 $\pm$ 0.005	1.49 $\pm$ 0.04	12.56 $\pm$ 0.60	LV 123
core 5	179/179	13,300	500	feldspars	84 $\pm$ 9	4–15	1.66 $\pm$ 0.07	6.97 $\pm$ 0.17	1.62 $\pm$ 0.04	0.06 $\pm$ 0.004	1.52 $\pm$ 0.04	20.17 $\pm$ 0.98	LV 122
core 6	905.25/1165.75	53,000	3,000	feldspars	33 $\pm$ 7	4–15	2.79 $\pm$ 0.13	6.78 $\pm$ 0.56	1.38 $\pm$ 0.03	0.06 $\pm$ 0.003	2.31 $\pm$ 0.1	122 $\pm$ 5	LV 124
core 12	981	7,400	500	feldspars	88 $\pm$ 9	4–15	2.86 $\pm$ 0.16	6.08 $\pm$ 0.64	1.62 $\pm$ 0.04	0.08 $\pm$ 0.01	1.75 $\pm$ 0.05	12.95 $\pm$ 0.68	LV 127
core 12	1430	11,300	600	feldspars	84 $\pm$ 9	4–15	1.77 $\pm$ 0.07	5.70 $\pm$ 0.17	1.44 $\pm$ 0.04	0.06 $\pm$ 0.004	1.69 $\pm$ 0.06	15.62 $\pm$ 0.66	LV 125
core 12	1882	7,500	400	feldspars	48 $\pm$ 7	4–15	2.12 $\pm$ 0.16	5.18 $\pm$ 0.62	1.18 $\pm$ 0.04	0.07 $\pm$ 0.01	1.69 $\pm$ 0.06	12.72 $\pm$ 0.59	LV 126

showing a homogenous silica concentration of ca 70.6 wt% (normalized data), relatively high  $\text{Al}_2\text{O}_3$  concentrations (14.9–15.6 wt%), and a  $\text{K}_2\text{O}/\text{Na}_2\text{O}$  ratio of ca 0.6. The secondary glass component displays a rhyolitic composition with relatively high silica (77.7 wt%) and potassium concentrations (3.4 wt%, Table 3). Minerals are rare and comprise plagioclase, orthopyroxene, amphibole and apatite phenocrysts. Sporadically, corroded xenocrysts of quartz, biotite and clinopyroxene occur most likely representing components of granodioritic rock fragments. The t5–8 tephra is geochemically and mineralogical similar to tephra t6–4, at 379 cm sediment depth in core 6, deposited directly below the unconformity (Figs. 2, 4 and 6). Therefore it is attributed to an older eruption of Reclús volcano during OIS 3 (Haberzettl et al., 2008).

Geochemical tephra analyses show that tephra t5–2b and t12–22 (younger Reclús tephra) as well as t5–8 and t6–4 (older Reclús tephra) originate from two eruptions of the same volcano (Fig. 6). Therefore, the first pair can be used to date the upper section of profile 5 + 6. The second pair can be used to link core 5 to core 6 (Figs. 3 and 4).

Tephra t5–1, 78 cm and t5–2a, 96 cm from the upper section of core 5 resemble petrographically and stratigraphically tephra t12–12, 1075 cm and t12–15, 1320 cm in core 12 and therefore have been allocated to the Hudson eruption (8100 cal BP) and the Mt Burney eruption (8680 cal BP), respectively (Fig. 4). Tephra results of the three cores 5, 6, and 12 indicate that volcanic ashes were at least in the northern part of Laguna Potrok Aike homogeneously deposited.

#### 4.2. Lithologies and age-depth modeling

The 740 cm long sediment core 5 consists of homogeneous grey lacustrine mud with grain sizes ranging from clay to fine sand intercalated with volcanic ash layers. The correlation of cores 5 and 6 is based on the results of tephrochronological investigations and comparisons of  $k$  in concert with the visual correlation of high resolution digital photographs of the two cores (Fig. 7) as well as on seismic profiles (Fig. 2). Both cores were merged into a composite record (profile 5 + 6) taking advantage of the tephra layers t5–2b and t6–4 as most prominent marker horizons for the catenation (Fig. 4). The lower part of core 6 (below 379 cm in core 6) was used for the bottom whereas the uppermost part of core 5 provided the top of the composite section (surface to 640 cm depth, both in core 5 and profile 5 + 6). Comparisons of  $k$  profiles and the photographs of cores 5 and 6 indicate similar sedimentation rates for core 5 and core 6 below t6–4 (Fig. 7) which means below the hiatus, as t6–4 provides the first evidence for undisturbed deposition below the hiatus (Haberzettl et al., 2008).

The age-depth model for profile 5 + 6 was established by linear interpolation of radiocarbon ages of tephra identified in core 5 and the radiocarbon date of 48 500  $\pm$  2525 cal BP obtained from core 6 (Table 1, Fig. 3). No other material for radiocarbon dating was available to further refine the chronology. The complete profile 5 + 6 is 1171 cm long and provides a continuous record of sedimentation spanning 55 ka (Fig. 3). This indicates that this

composite record continuously covers Oxygen Isotope Stage (OIS) 1 (Holocene) to OIS 3 (59–29 ka). Although the age model is rather coarse, the chronology of profile 5 + 6 already indicates variations in the sedimentation rate (Fig. 3): above the younger Reclús tephra (t5–2b) only minor variations occur except for the part between the Hudson (t5–1) and Mt Burney (t5–2a) tephra. Before the Mt Burney and after the Hudson tephra sedimentation rates are similar ( $0.1 \text{ mm a}^{-1}$ ) (Fig. 3). The same pattern was previously observed in core 12 from the centre of the lake (Fig. 5) and attributed to a low lake level enabling erosion of emerging lacustrine sediments (Haberzettl et al., 2007a; Anselmetti et al., 2009; Mayr et al., 2009). The latter might have also caused the higher sedimentation rates depicted in profile 5 + 6 although to a lesser degree than in the depocentre of the lake centre, because this record originates from the flanks of Laguna Potrok Aike (Fig. 2).

The age model of profile 5 + 6 points towards another change to higher sedimentation rates ( $0.3 \text{ mm a}^{-1}$ ) below the younger Reclús tephra (t5–2b, 142.5 cm sediment depth). This may indicate a change in sediment availability or a change in the mode of sediment transport. The hitherto undated tephra layers included in this section of higher sedimentation rates show ages of 34 ka (Reclús t5–8/t6–4), 45 ka (Mt Burney t6–8) and 54 ka (also Mt Burney t6–10) and were all deposited during OIS 3 (Fig. 3).

The age-depth model of core 12 (Fig. 5) using calibrated radiocarbon dates and the same tephra layers was already discussed before (Haberzettl et al., 2007a). In order to obtain comparable age-depth models, only calibrated  $^{14}\text{C}$  dates were used to build up chronologies. The absence of a reservoir effect in Laguna Potrok Aike at least for the past 16 000 cal BP was previously demonstrated by  $^{14}\text{C}$ -dating of modern aquatic plants and the total inorganic carbon fraction of a number of bulk samples distributed all over the record. Many different materials (terrestrial and aquatic) were used for

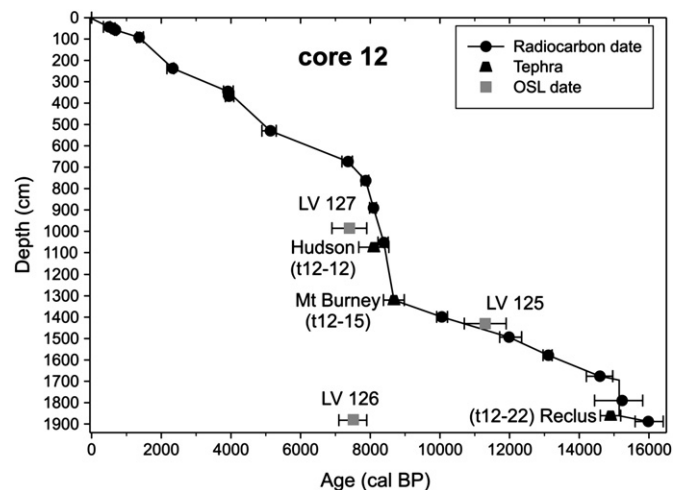


Fig. 5. Age-depth model of core 12. OSL ages are plotted for comparison.

**Table 3**

Mean major element oxide concentrations (normalized data) of glass shards extracted from tephra layers t5-2 and t5-8.  $n$  = number of shards analyzed. 1 $\sigma$  standard deviations are shown as numbers in parentheses.

	t5-2		t5-8	
	glass a	glass b	glass a	glass b
SiO <sub>2</sub>	76.81 (0.51)	66.71	70.58 (0.19)	77.72
TiO <sub>2</sub>	0.18 (0.12)	0.27	0.64 (0.24)	0.05
Al <sub>2</sub> O <sub>3</sub>	12.94 (0.22)	17.46	15.29 (0.26)	13.14
FeO	1.25 (0.06)	3.60	2.80 (0.10)	1.10
MnO	0.07 (0.05)	0.08	0.07 (0.02)	0.00
MgO	0.21 (0.02)	1.69	0.83 (0.05)	0.17
CaO	1.51 (0.07)	4.82	3.16 (0.16)	1.29
Na <sub>2</sub> O	4.38 (0.63)	3.90	4.11 (0.28)	3.15
K <sub>2</sub> O	2.65 (0.09)	1.47	2.50 (0.10)	3.38
Total	100.00	100.00	100.00	100.00
	$n = 4$	$n = 1$	$n = 7$	$n = 1$

dating which resulted in a consistent age-depth model thus also minimizing the effect of incorporation of old organic carbon as it would be the case with bulk samples (Haberzettl et al., 2005, 2007a). OSL ages (Tables 1 and 2) were plotted only for comparison in/with the respective <sup>14</sup>C age model (Figs. 3 and 5).

#### 4.3. OSL dating

The optical ages from core 12 and from profile 5 + 6 in most cases show a slight offset to the age-depth model which is based on median ages of calibrated radiocarbon dates (Figs. 3 and 5). In core 12 (Fig. 5) one date at 1430 cm sediment depth (LV 125) matches the age-depth model. The OSL ages at 981 cm (LV 127) and 1882 cm (LV 126) show an offset of ~850 years and 8300 years, respectively. In the upper part of profile 5 + 6 the OSL ages of LV 122 and LV 123 are in correct stratigraphic order but also in slight offset to the radiocarbon age model (see younger Reclús, Hudson and Mt Burney tephra, Fig. 3). With increasing age (sample LV 124 at the bottom of

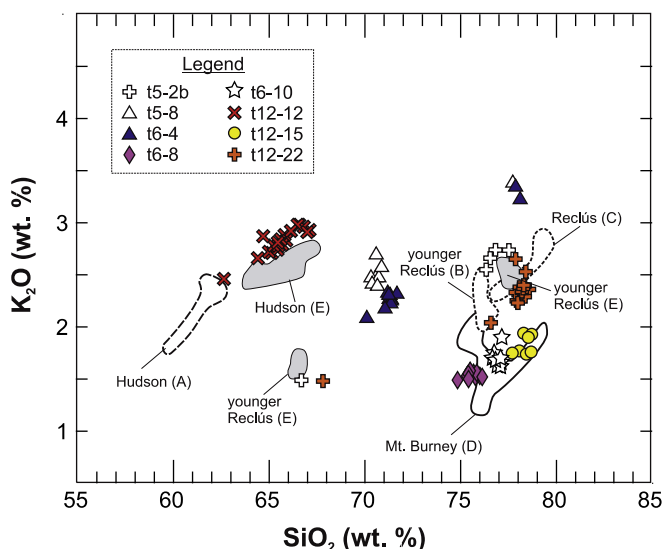


**Fig. 6.** Geochemical characterization (silica versus potassium of normalized data) of glass shards of tephra layers from Laguna Potrok Aike showing that t5-2b and t12-22 as well as t5-8 and t6-4 are geochemically identical. Volcanic glass data of proximal correlatives (white fields) and distal tephra layers from Lago Cardiel (grey fields) are plotted for comparison. Data from: (A) Naranjo and Stern (1998), Kilian et al. (2003); (B) Stern (1990); (C) Kilian et al. (2003); (D) Stern (1990), Kilian et al. (2003); (E) Lago Cardiel: Haberzettl et al. (2007a), this study.

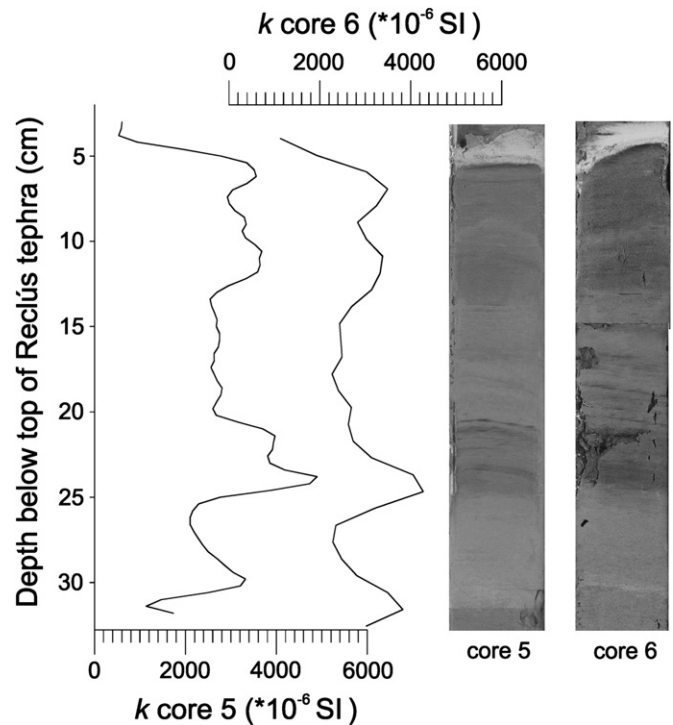


**Fig. 7.** Comparison of magnetic susceptibility ( $k$ ) records and photographs of core 5 and core 6 below the isochronous marker layer (older Reclús tephra) showing good correlation. As data for  $k$  of core 5 was measured in 4 mm resolution and data for core 6 in 1 cm resolution, data for core 5 was smoothed with a 3-point moving average in order to make records comparable to each other.

profile 5 + 6) the offset disappears due to increasing error of the dating methods (Fig. 3).

#### 4.4. Geochemical and geophysical data

Fig. 8 shows the combined magnetic susceptibility ( $k$ ) as well as the combined Ca/Ti ratio curves for profile 5 + 6 converted to a time scale. The oldest sediments of profile 5 + 6 show constant but low Ca/Ti values. This ratio is higher in the upper part with distinct peaks at 8, 4, 0.5 and 0.1 cal ka BP. Conversely,  $k$  exhibits an opposite pattern: low values with minor peaks during the Holocene are followed by much higher values during OIS 2 and 3 (only visible before 16 cal ka BP in Fig. 8). From 38 to 33 cal ka BP, the magnetic susceptibility values are comparatively low although not as low as during the Holocene (Fig. 8). The interval between 33 and 17 cal ka BP displays high  $k$  values with some kind of cyclical pattern as shown by minima at 28, 23 and 19 cal ka BP. Missing element ratios and  $k$  values are a sampling artefact since the cores were sampled for other purposes prior to the measurement of these parameters.

A comparison of the Ca variations during the past 9000 cal BP between core 5 and core 12 (centre of the lake) as well as core 6 (above the unconformity) allows to correlate the main peaks (Fig. 9). Different units are caused by the use of different XRF-scanners. The slight time shift between the intervals yielding high Ca values in the different cores during the Medieval Climate Anomaly (Stine, 1998; Haberzettl et al., 2005) is most probably due to the short duration of this interval and age interpolation errors due to the absence of radiocarbon dates from cores 5 and 6 close to this period (Fig. 9). Moreover, in the individual Ca records of cores 5 and 6 (Fig. 9) and in the Ca/Ti ratio of profile 5 + 6 (Fig. 8) an additional peak can be observed between 4500 and 4000 cal BP which is ambiguous in core 12 (Fig. 9).

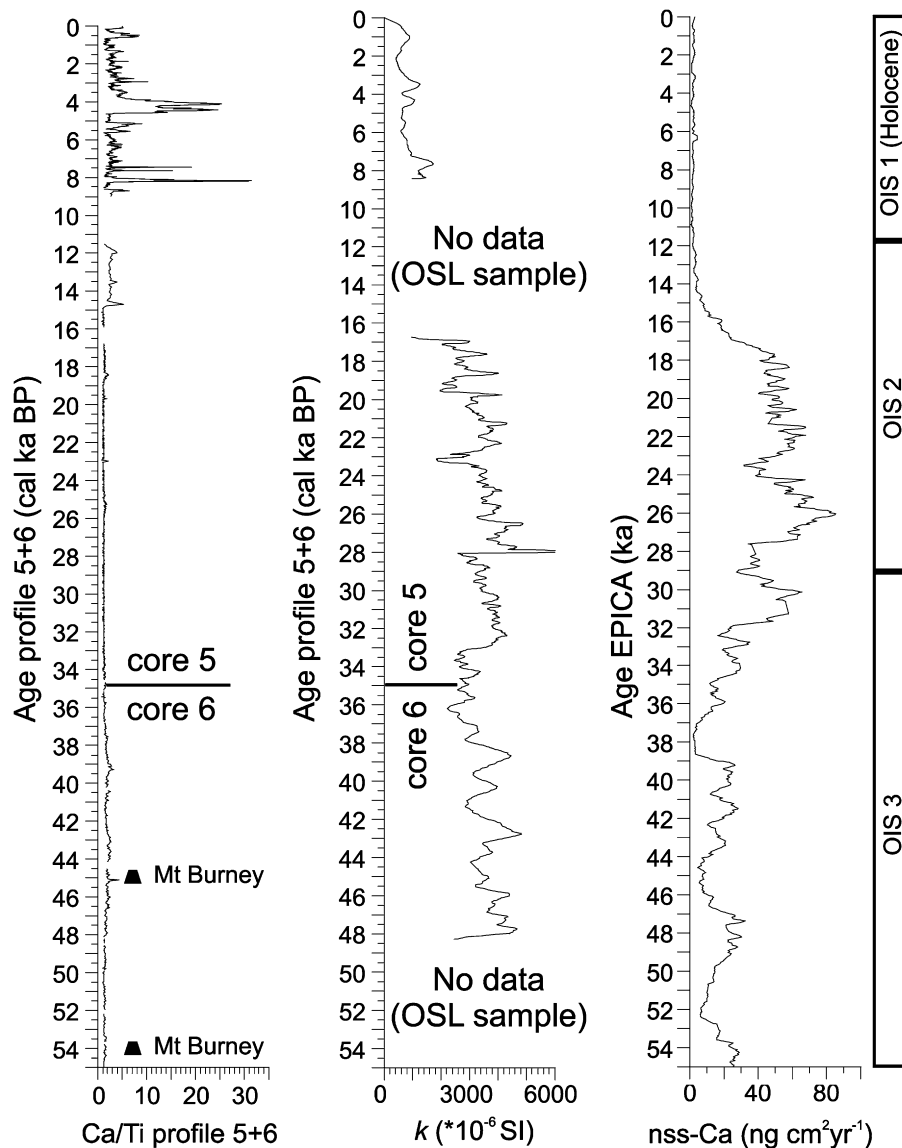


**Fig. 8.** Ca/Ti ratios and magnetic susceptibility data ( $k$ ) from profile 5 + 6 plotted vs. time (left, center). The non-sea-salt calcium (nss-Ca) flux from the Dome C ice core record from Antarctica (right, Röthlisberger, 2005) is plotted for comparison with the  $k$  record from Laguna Potrok Aike. The bars on the right refer to the climatic stage of the different chronostratigraphic units. Data for  $k$  of core 5 is smoothed with a 11-point moving average and for nss-Ca with a 3-point moving average. Different moving averages were used to account for different resolutions of data points. Missing sections of the  $k$  record are related to gaps resulting from prior sampling for other parameters. Locations of Mt Burney tephra layers (trapezes) were indicated in core 6 for comparison. The line separating core 5 and core 6 is the older Reclús tephra (correlating marker layer).

## 5. Discussion

### 5.1. Dating

Except for sample LV 126 all optical dates approximate the ages determined by  $^{14}\text{C}$  dating and the disappearing offsets for older sediments imply that optical dating is a promising tool for dating sediments of Laguna Potrok Aike exceeding the radiocarbon dating range. The slight offset between radiocarbon and optical ages maybe caused by one or several factors: (i) different sampling positions, (ii) old organic carbon incorporated in plants used for radiocarbon dating, (iii) anomalous fading of the feldspar-derived OSL signal (Wintle, 1973) leading to an underestimation of the true age. It is therefore likely that the true chronology of the lake sediments is situated in between the OSL- and the radiocarbon-derived data points. The sample LV 126, however, remains a hard to explain outlier. Even if we account for

anomalous signal fading (usually 20%) and underestimated water content, the age of the sample would not exceed  $\sim 12$  ka, an age which still underestimates the radiocarbon age of the Reclús tephra.

For younger sediments, as the covered time period of this study radiocarbon ages are more precise. For this and the following reasons we stick to these calibrated dates for age modeling: (a) In earlier studies the absence of a reservoir effect was demonstrated for the past 16 000 cal BP for the sediments of Laguna Potrok Aike (Haberzettl et al., 2005, 2007a), (b) no carbonates which could be transported to the lake during times of increased precipitation (rain or snow) were found in the catchment area (Haberzettl et al., 2005), (c) OSL ages show an offset for time intervals for which the radiocarbon ages are in agreement with other regional archives (Haberzettl et al., 2007a), indicating that OSL slightly underestimates the true ages in younger sediments from Laguna Potrok Aike.

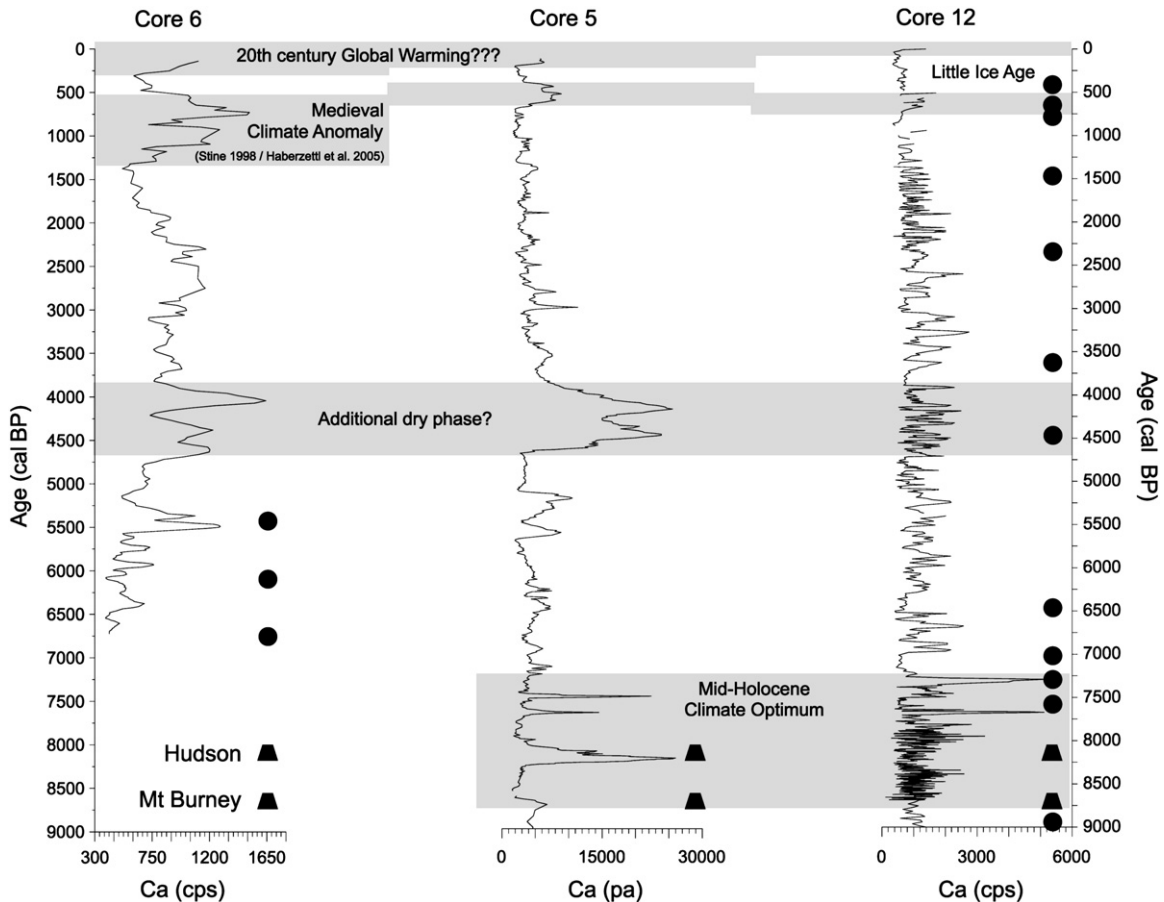


**Fig. 9.** Comparison of Ca records (cps: counts per second, pa: peak area) from the flanks (core 5 and core 6) and the center of Laguna Potrok Aike (core 12) showing correlations except for ca 4 cal ka BP. Dots indicate calibrated radiocarbon dates in the individual records whereas trapezoids indicate locations of Hudson and Mt Burney tephras found in cores 5 and 12. Please note that due to the use of different XRF-scanners ranges are different.

### 5.2. Indicators for lake level variations

Earlier studies have allocated high values of Ca to the precipitation of autochthonous calcite (Haberzettl et al., 2005, 2007a). Due to ion concentration and dilution effects in the water column, calcite precipitation provides a qualitative estimation for lake-level variations. Low Ca values are indicative for a rising or high lake-level whereas high Ca values indicate a falling or low lake-level (Haberzettl et al., 2008). It was also demonstrated for Laguna Potrok Aike that Ti is associated with allochthonous input resulting from runoff and hence, reflecting hydrological variability (Haberzettl et al., 2005, 2007a). Therefore, Ti can be used as a complementary indicator for lake level fluctuations. Potentially, there might be some loss of fluviially derived matter during overflow situations. This would be caused by a loss of at least parts of suspended material through the outflow rather than deposition in the lake (Haberzettl et al., 2007a). Following these considerations concerning Ca and Ti, the Ca/Ti ratio in Laguna Potrok Aike sediments reflects hydrological variability with high values during drier phases and low values responding to times of increased moisture availability.

### 5.3. Hydrological reconstruction of the past 55 ka

The Ca/Ti ratios of profile 5 + 6 indicate a variable lake level during the Holocene with punctuated regressions at 8, 4, 0.5 and 0.1 cal ka BP (Fig. 8). Three of these four phases were previously detected in sediment core 12 from the centre of the lake using

a multi-proxy approach (Haberzettl et al., 2005, 2007b; Wille et al., 2007; Mayr et al., 2009) and are highlighted in Fig. 9. These were attributed to the Mid-Holocene Climate Optimum, the Medieval Climate Anomaly and the 20th Century Global Warming, respectively (Haberzettl et al., 2005, 2007a). The new long records recovered from Laguna Potrok Aike (Fig. 9) imply that on a longer timescale the dry phase of the Medieval Climate Anomaly is not as exceptional as previously assumed based on shorter records (Haberzettl et al., 2005). However, it remains a distinct feature present in all cores. Although the age-depth models of the Holocene sections in cores 5 and 6 are only based on linear interpolation of a few ages, the Ca content allows the correlation of the main events. This indicates consistent sedimentation patterns for the three coring locations. The Ca peak at 4 cal ka BP, however, is only found in the littoral, i.e., in core 5 and core 6 (Figs. 2 and 9). Sedimentation rates for core 12 increased during that period in the centre of the lake (Fig. 5). Considering that sedimentation rates increased in all cores during the sharp lake level drop at 8 cal ka BP due to erosion of formerly submerged littoral areas (Haberzettl et al., 2007b, 2008; Mayr et al., 2009), the increase of profundal sedimentation rates around 4 cal ka BP (Fig. 5) might also be related to a lake level lowering. Such a reworking of former littoral sediments containing no or only little amounts of calcite as they were deposited during a lake-level high stand, would also lead to a dilution of the autochthonously precipitated calcite in the centre of the lake. Furthermore, warmer waters in the shallower areas of littoral cores 5 and 6 might favour calcite precipitation resulting in a more pronounced signal here compared to the centre of the lake.

As the increase in sedimentation rates in the centre (core 12) around 4 cal ka BP is not as pronounced as at 8 cal ka BP (Fig. 5) the Ca peak in cores 5 and 6 can probably be associated with a minor lake level lowering already postulated through seismic sequence analysis of submerged paleoshorelines at 16 to 17 m below modern lake level (Anselmetti et al., 2009).

The Ca/Ti ratio indicates dominant high lake levels during both OIS 3 and 2 (Fig. 8) with an associated overflow that contrast the today's terminal lake character of the basin. This might have led to reduced ionic concentrations, i.e., no calcite precipitation during the pre Holocene. However, during these periods the interpretation of Ca/Ti ratios as a sensitive hydrological proxy is complicated since it only indicates a high lake level for the entire time interval. This scenario does not necessarily imply higher precipitation (rain and snow), as due to lower global temperatures evaporation was certainly reduced during the glacial as well. A reconstruction of varying west wind strength during the glacial similar as it has been done for the Holocene (Mayr et al., 2007b) cannot be deduced from long-distance transported pollen due to different vegetation cover (Wille et al., 2007). The impact of varying west wind strength to this hydrological system during the glacial hence remains speculative. Despite these restrictions, the Ca/Ti ratios indicate a positive water balance for Laguna Potrok Aike for glacial conditions (i.e., after 55 ka).

#### 5.4. Aeolian input

Similarities were found between the independently dated magnetic susceptibility ( $k$ ) record from Laguna Potrok Aike and the non-sea-salt calcium (nss-Ca) flux from the EPICA Dome C ice core record (75°06'S, 123°24'E, Fig. 1, 8) (Röthlisberger, 2005) the latter being a proxy for mineral dust deposition in Antarctica (Röthlisberger et al., 2002, 2004). During the last glacial period, considerable variation of dust is observed in this record, pointing to climatic changes in southern South America, an area which has been considered to be the main dust source for Dome C (Delmonte et al., 2008). Within the precision of the age models, similarities exist for full glacial conditions (in this case 17–32/33 cal ka BP). During this time values of both records are high and show contemporaneous reductions at ~23 and ~28 cal ka BP. Similar agreement is found for the minimum before, starting at ca 38/39 cal ka BP and for the three peaks between 38/39 and ~44 cal ka BP. Considering the precision of the age model of Laguna Potrok Aike potentially the three minor peaks topping a maximum at the onset of the record of profile 5 + 6 around 46–49 cal ka BP (Fig. 8) correlate as well.

Similar analogies were found between downcore variations in magnetic susceptibility of marine sediment cores from the Scotia Sea (Fig. 1) located southwest of Patagonia and concentration as well as dust flux in East Antarctic ice cores (Hofmann, 1999; Pugh et al., 2009). However, the correlation diminishes close to continental margins, i.e., close to sources of glacial debris and regions affected by gravitational downslope transport. Although, the authors have not established the precise cause of this correlation as the physical basis for the relationship at present remains unclear, its validity also around the circum-Antarctic west wind belt suggests that the material was either transported by wind or supplemented by wind-driven current transport (Pugh et al., 2009).

As wind driven ocean current transport can be ruled out in the record from Laguna Potrok Aike the cause for similar patterns of  $k$  and nss-Ca from Dome C must be different. Magnetic susceptibility was previously assumed to indicate aeolian input to Laguna Potrok Aike (Haberzettl et al., 2008). Sediments deposited during glacial times mainly consist of well-sorted coarse silt and fine sand (20–200  $\mu\text{m}$ , Fig. 10) in contrast to the more organic and calcite

dominated Holocene counterpart with a less sorted grain size distribution (Fig. 10) (Haberzettl et al., 2008). This grain size fraction dominating glacial sediments of Laguna Potrok Aike is one of the first fractions to be moved by wind and kept in suspension (Tucker, 1991). Therefore, the well sorted sediments indicate aeolian transport as the dominant agent ruling sedimentation during glacial times.

As it varies with magnetite grain size,  $k$  usually shows a distinct maximum between 25 and 100  $\mu\text{m}$  (Dearing, 1994). The latter closely matches the peaks in grain-size distributions of the sediments deposited in Laguna Potrok Aike during glacial times (Fig. 10) when in contrast to the Holocene values of  $k$  are increased by one order of magnitude (Haberzettl et al., 2008). This difference in  $k$ , between glacial and Holocene times, in concert with the contemporaneous change in grain size distribution as well as the dependency of  $k$  on grain size (Dearing, 1994) might suggest a causal relationship between these two parameters also for the sediments of Laguna Potrok Aike.

Assuming that for Laguna Potrok Aike  $k$  is an indicator of aeolian input, dust (aeolian transport) deposition was much higher during glacial times compared to the Holocene. This assumption is further enforced by the comparatively higher sedimentation rates observed during OIS 3 and 2 (Fig. 3). As  $k$  is measured volumetrically, more or magnetically higher susceptible material has to be included in the sediments in order to obtain higher values in the same volume. Although potentially there might have been an increased discharge inferred from the Ca/Ti ratio during the glacial period this would have contributed to a coarsening of the grain size distribution in the center of the lake but probably not in the littoral where profile 5 + 6 was recovered. Additional support comes from the grain size distribution itself showing a much better sorting that indicates proportionally less clay and silt contribution during the glacial than during the Holocene (Fig. 10).

Unfortunately, it remains unclear whether the intensity of the high  $k$  values between 38/39 and 44 cal ka BP is an artifact of the use of two different sensors of the same type or if the intensity is indeed as high as during the Last Glacial Maximum (LGM) which opposes the lower nss-Ca values in Dome C during that time. Additional to the effects of different grain-size distributions, the difference in  $k$  between the Holocene and earlier times might be influenced by the presence of calcite and/or organic matter in the youngest section, since both calcite and organic matter are diamagnetic (Hall et al., 2001). However, comparisons of  $k$  vs. TIC (total inorganic carbon) and  $k$  vs. TOC (total organic carbon) in other cores from Laguna Potrok Aike, in which calcite and organic matter are present, show no correlation between  $k$  and TIC

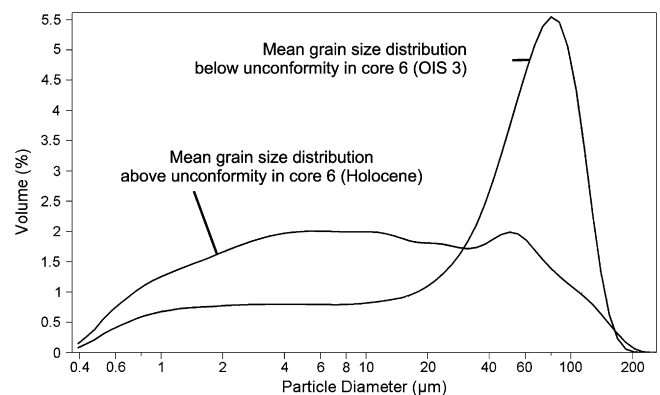


Fig. 10. Mean grain size distribution above (OIS 1: Holocene) and below (OIS 3) the hiatus in core 6 (after Haberzettl et al., 2008).

( $R^2 = 0.07$ ) or TOC ( $R^2 = 0.02$ ) (Haberzettl et al., 2007a). Sediments below the unconformity in core 6 yield TIC values below detection limits which prevents a correlation. These sediments further give a correlation of  $R^2 = 0.07$  for TOC vs.  $k$ , confirming a negligible influence of calcite and organic matter on  $k$  during glacial times (Haberzettl et al., 2008).

Alternatively, aeolian transport might provide sediments of different provenance, potentially bearing higher magnetic susceptibility. This might for example be associated with an additional glacial source which is not active during the Holocene (Ackert, 2009; Sugden et al., 2009) when the  $k$  signal is lower. Studies in marine sediment cores from mid latitudes in the South Indian Ocean, eastward of the Kerguelen Islands (Fig. 1) show that magnetic susceptibility is not related to variations in grain sizes but reflects changes in the flux of magnetite (Mazaud et al., 2007). Although the authors do not discuss their results in terms of aeolian input magnetic susceptibility profiles strongly resemble variations in Antarctic dust concentrations (Dezileau et al., 2000; Mazaud et al., 2007; Pugh et al., 2009). Potentially, in Laguna Potrok Aike grain size could only act as an indicator for aeolian activity but changes in the magnetic susceptibility signal might also be enhanced or solely related to changes in the flux of highly susceptible material. However, the existence and exact role of these potential contributions have to be further explored in future studies.

Changes in grain size (Haberzettl et al., 2008) as well as the higher  $k$  found during glacial times in sediments of Laguna Potrok Aike either imply a) stronger westerly winds leading to intensified deflation and improved transport conditions; b) favoured conditions for wind erosion for example due to reduced vegetation cover (Wille et al., 2007) or (peri-)glacial processes (Ackert, 2009; Sugden et al., 2009); or c) a combination of both. A relatively open vegetation during the Lateglacial due to lower temperatures was previously suggested for the investigated environment (Wille et al., 2007). Investigations in the region surrounding the Strait of Magellan (Fig. 1) also show that dust peaks in Antarctica coincide with periods when rivers of glacial meltwater deposited sediment onto outwash plains from where it could easily be mobilized by wind (Sugden et al., 2009). Lake level reconstructions for Lago Cardiel (morphometrically different and located 350 km north of Laguna Potrok Aike) indicate dry conditions during the Last Glacial Maximum (Gilli et al., 2001) coinciding with an enhanced Patagonian dust deposition on the Antarctic ice-shield (Yung et al., 1996). Furthermore, GCM simulations show that atmospheric transport potentially carrying dust from Patagonia to Antarctica was faster during the Last Glacial Maximum (Krinner and Genthon, 2003). All these evidence suggest that the scenario proposed from Laguna Potrok Aike is realistic. The ultimate reason for the dust increase during glacial times, however, cannot be solved from this record alone.

Possibly magnetic susceptibility could be used to transfer an ice core age model to the sediments recovered within the ICDP (International Continental Scientific Drilling Program) project PASADO (Potrok Aike maar lake Sediment Archive Drilling project) as it was proposed for marine sediments in the Scotia Sea (Pugh et al., 2009). This would give additional time control to the anticipated radiocarbon, OSL, tephrochronology and stratigraphic efforts (paleomagnetism, pollen, stable isotopes).

## 6. Conclusions

Sediment core 5 from Laguna Potrok Aike closes the gap caused by a hiatus in littoral core 6. The combination of both cores allowed to produce the composite profile 5 + 6 containing a continuous paleoenvironmental record for the past 55 ka. The latter is unique

for the southern Patagonian steppe, an area with no comparable continuous records covering that age range so far. Refining the Holocene record, a sharp increase in calcite was detected in the littoral cores. This augmentation in autochthonous carbonate precipitation is ascribed to a minor lake level lowering dated to 4.5 to 4 cal ka BP and possibly related to a submerged paleoshoreline at 16/17 m below today's lake level. Apart from this peak in Ca, the records of this element and the tephra indicate a similar sedimentation pattern for the three coring sites. During glacial times a very high lake level indicates a positive hydrological balance which probably triggered an overflow of the lake. In accordance with the Dome C ice core record from Antarctica, aeolian transport in Patagonia itself was more vigorous during glacial times than during the Holocene. This is the first evidence for temporally similar dust deposition patterns in Antarctica and in the main source area of Patagonia. In concert with OSL dates magnetic susceptibility might be used to provide chronological information (transfer of ice core age model) for the extension of the record back in time using the sediment records recovered in the ICDP (International Continental Scientific Drilling Program) deep drilling project PASADO (Potrok Aike maar lake Sediment Archive Drilling project). OSL dates from Laguna Potrok Aike show a good approximation to radiocarbon ages in older sediments where both dating methods delivered the smallest difference.

## Acknowledgements

We thank Regine Röthlisberger for providing us with her non-sea-salt calcium data from Dome C. Sabine Stahl and Ellen Reid are acknowledged for assistance with geochemical and tephra analyses as well as Guillaume St-Onge for comments on parts of an earlier draft of this manuscript. Raimon Tolosana-Delgado, Hilmar von Eynatten, Hans Ruppert, István Dunkl and Volker Karius provided fruitful discussions. We also acknowledge the helping hands of Philipp Bluszcz during core processing. Finally, we would like to thank Barbara Delmonte and an anonymous reviewer for their substantial comments which improved an earlier version of the manuscript distinctively. This is a contribution to the German Climate Research Program DEKLIM (grants 01 LD 0034 and 0035) of the German Federal Ministry of Education and Research (BMBWF). Seismic surveys were funded by the German Research Foundation (DFG Zo102/5-1, 2, 3) in the framework of the priority program ICDP. Torsten Haberzettl is currently supported by a postdoctoral fellowship scholarship provided by Le Fonds québécois de la recherche sur la nature et les technologies (FQRNT). This constitutes GEOTOP contribution n° 2009-0017.

## References

- Ackert, R.P.J., 2009. Palaeoclimate: Patagonian dust machine. *Nature Geoscience* 2, 244–245.
- Anselmetti, F.S., Ariztegui, D., Batist, M.D., Gebhardt, A.C., Haberzettl, T., Niessen, F., Ohlendorf, C., Zolitschka, B., 2009. Environmental history of southern Patagonia unravelled by the seismic stratigraphy of Laguna Potrok Aike. *Sedimentology* 56, 873–892.
- Basile, I., Grousset, F.E., Revel, M., Petit, J.R., Biscaye, P.E., Barkov, N.I., 1997. Patagonian origin of glacial dust deposited in East Antarctica (Vostok and Dome C) during glacial stages 2, 4 and 6. *Earth and Planetary Science Letters* 146, 573–589.
- Corbella, H., 2002. El campo volcano-tectónico de Pali Aike. In: Haller, M. (Ed.), *Geología y Recursos Naturales de Santa Cruz*. Asociación Geológica Argentina, Buenos Aires, pp. 285–302.
- Croudace, I.W., Rindby, A., Rothwell, R.G., 2006. ITRAX: description and evaluation of a new multi-function X-ray core scanner. In: Rothwell, R.G. (Ed.), *New Techniques in Sediment Core Analysis*. Geological Society, London, pp. 51–63.
- D'Orazio, M., Agostini, S., Mazzarini, F., Innocenti, F., Manetti, P., Haller, M.J., Lahsen, A., 2000. The Pali Aike Volcanic Field, Patagonia: slab-window magmatism near the tip of South America. *Tectonophysics* 321, 407–427.
- Dearing, J., 1994. *Environmental Magnetic Susceptibility*. Using the Bartington MS2 System. Chi Publishing, Kentworth.

- Delmonte, B., Basile-Doelsch, I., Petit, J.R., Maggi, V., Revel-Rolland, M., Michard, A., Jagoutz, E., Grousset, F., 2004. Comparing the Epica and Vostok dust records during the last 220,000 years: stratigraphical correlation and provenance in glacial periods. *Earth-Science Reviews* 66, 63–87.
- Delmonte, B., Andersson, P.S., Hansson, M., Schönberg, H., Petit, J.R., Basile-Doelsch, I., Maggi, V., 2008. Aeolian dust in East Antarctica (EPICA-Dome C and Vostok): provenance during glacial ages over the last 800 kyr. *Geophysical Research Letters* 35, L07703. doi:10.1029/2008GL033382.
- Dezileau, L., Bareille, G., Reyss, J.L., Lemoine, F., 2000. Evidence for strong sediment redistribution by bottom currents along the southeast Indian ridge. *Deep Sea Research Part I: Oceanographic Research Papers* 47, 1899–1936.
- Endlicher, W., 1993. Klimatische Aspekte der Weidedegradation in Ost-Patagonien. In: Hornetz, B., Zimmer, D. (Eds.), Beiträge zur Kultur- und Regionalgeographie. Festschrift für Ralph Jätzold. *Trierer Geographische Studien. Geographische Gesellschaft Trier, Trier*, pp. 91–103.
- Gilli, A., Anselmetti, F., Ariztegui, D., Bradbury, J., Kelts, K., Markgraf, V., McKenzie, J., 2001. Tracking abrupt climate change in the Southern Hemisphere: a seismic stratigraphic study of Lago Cardiel, Argentina (49°S). *Terra Nova* 13, 443–448.
- Gilli, A., Anselmetti, F.S., Ariztegui, D., Beres, M., McKenzie, J.A., Markgraf, V., 2005a. Seismic stratigraphy, buried beach ridges and contourite drifts: the Late Quaternary history of the closed Lago Cardiel basin, Argentina (49°S). *Sedimentology* 52, 1–23.
- Gilli, A., Ariztegui, D., Anselmetti, F.S., McKenzie, J.A., Markgraf, V., Hajdas, I., McCulloch, R.D., 2005b. Mid-Holocene strengthening of the Southern Westerlies in South America – sedimentological evidences from Lago Cardiel, Argentina (49°S). *Global and Planetary Change* 49, 75–93.
- Haberzettl, T., 2006. Late Quaternary Hydrological Variability in Southeastern Patagonia – 45,000 Years of Terrestrial Evidence from Laguna Potrok Aike. PhD thesis University of Bremen. <http://nbn-resolving.de/urn:nbn:de:gbv:46-diss000103918>.
- Haberzettl, T., Fey, M., Lücke, A., Maidana, N., Mayr, C., Ohlendorf, C., Schäbitz, F., Schleser, G.H., Wille, M., Zolitschka, B., 2005. Climatically induced lake level changes during the last two millennia as reflected in sediments of Laguna Potrok Aike, southern Patagonia (Santa Cruz, Argentina). *Journal of Paleolimnology* 33, 283–302.
- Haberzettl, T., Wille, M., Fey, M., Janssen, S., Lücke, A., Mayr, C., Ohlendorf, C., Schäbitz, F., Schleser, G., Zolitschka, B., 2006. Environmental change and fire history of southern Patagonia (Argentina) during the last five centuries. *Quaternary International* 158, 72–82.
- Haberzettl, T., Corbella, H., Fey, M., Janssen, S., Lücke, A., Mayr, C., Ohlendorf, C., Schäbitz, F., Schleser, G.H., Wille, M., Wulf, S., Zolitschka, B., 2007a. Lateglacial and Holocene wet-dry cycles in southern Patagonia: chronology, sedimentology and geochemistry of a lacustrine record from Laguna Potrok Aike, Argentina. *The Holocene* 17, 297–310.
- Haberzettl, T., Mayr, C., Wille, M., Zolitschka, B., 2007b. Linkages between Southern Hemisphere Westerlies and hydrological changes in semi-arid Patagonia during the last 16,000 years. *PAGES News* 15, 22–23.
- Haberzettl, T., Kück, B., Wulf, S., Anselmetti, F., Ariztegui, D., Corbella, H., Fey, M., Janssen, S., Lücke, A., Mayr, C., Ohlendorf, C., Schäbitz, F., Schleser, G.H., Wille, M., Zolitschka, B., 2008. Hydrological variability in southeastern Patagonia and explosive volcanic activity in the southern Andean Cordillera during Oxygen Isotope Stage 3 and the Holocene inferred from lake sediments of Laguna Potrok Aike, Argentina. *Palaeogeography, Palaeoclimatology, Palaeoecology* 259, 213–229.
- Hall, F.R., Andrews, J.T., Kerwin, M., Smith, L.M., 2001. Studies of sediment colour, whole-core magnetic susceptibility, and sediment magnetism of the Hudson Strait-Labrador Shelf region: CSS Hudson cruise 90023 and 93034. In: MacLean, B. (Ed.), *Marine Geology of Hudson Strait and Ungava Bay, Eastern Arctic Canada: Late Quaternary Sediments, Depositional Environments, and Late Glacial-Deglacial History Derived from Marine and Terrestrial Studies*. Geological Survey of Canada Bulletin, vol. 566, pp. 161–170.
- Hofmann, A., 1999. Kurzfristige Klimaschwankungen im Scotiameer und Ergebnisse zur Kalbungsgeschichte der Antarktis während der letzten 200 000 Jahre. Rapid Climate Oscillations in the Scotia Sea and Results of the Calving History of Antarctica During the Last 200000 Years (Berichte zur Polarforschung 345). PhD thesis, University of Bremen.
- Jansen, J.H.F., Van der Gaast, S.J., Kloster, B., Vaars, A.J., 1998. CORTEX, a shipboard XRF-scanner for element analyses in split sediment cores. *Marine Geology* 151, 143–153.
- Kaplan, M.R., Moreno, P.I., Rojas, M., 2008. Glacial dynamics in southernmost South America during Marine Isotope Stage 5e to the Younger Dryas chron: a brief review with a focus on cosmogenic nuclide measurements. *Journal of Quaternary Science* 23, 649–658.
- Kilian, R., Hohner, M., Biester, H., Wallrabe-Adams, H.J., Stern, C.R., 2003. Holocene peat and lake sediment tephra record from the southernmost Chilean Andes (53–55°S). *Revista Geologica de Chile* 30, 23–37.
- Krinner, G., Genhous, C., 2003. Tropospheric transport of continental tracers towards Antarctica under varying climatic conditions. *Tellus B* 55, 54–70.
- Mancini, M.V., Prieto, A.R., Paez, M.M., Schäbitz, F., 2008. Late quaternary vegetation and climate of patagonia. In: Rabassa, J. (Ed.), *Developments in Quaternary Science*. Elsevier, pp. 351–367.
- Markgraf, V., Bradbury, J.P., Schwalb, A., Burns, S.J., Stern, C., Ariztegui, D., Gilli, A., Anselmetti, F.S., Stine, S., Maidana, N., 2003. Holocene palaeoclimates of southern Patagonia: limnological and environmental history of Lago Cardiel, Argentina. *The Holocene* 13, 581–591.
- Mauz, B., Bode, T., Mainz, E., Blanchard, H., Hilger, W., Dikau, R., Zöller, L., 2002. The luminescence dating laboratory at the University of Bonn: equipment and procedures. *Ancient TL* 20, 53–61.
- Mayr, C., Fey, M., Haberzettl, T., Janssen, S., Lücke, A., Maidana, N.I., Ohlendorf, C., Schäbitz, F., Schleser, G.H., Struck, U., Wille, M., Zolitschka, B., 2005. Palaeoenvironmental changes in southern Patagonia during the last millennium recorded in lake sediments from Laguna Azul (Argentina). *Palaeogeography, Palaeoclimatology, Palaeoecology* 228, 203–227.
- Mayr, C., Lücke, A., Stichler, W., Trimborn, P., Ercolano, B., Oliva, G., Ohlendorf, C., Soto, J., Fey, M., Haberzettl, T., Janssen, S., Schäbitz, F., Schleser, G.H., Wille, M., Zolitschka, B., 2007a. Precipitation origin and evaporation of lakes in semi-arid Patagonia (Argentina) inferred from stable isotopes ( $\delta^{18}\text{O}$ ,  $\delta^2\text{H}$ ). *Journal of Hydrology* 334, 53–63.
- Mayr, C., Wille, M., Haberzettl, T., Fey, M., Janssen, S., Lücke, A., Ohlendorf, C., Oliva, G., Schäbitz, F., Schleser, G.H., Zolitschka, B., 2007b. Holocene variability of the Southern Hemisphere westerlies in Argentinean Patagonia (52°S). *Quaternary Science Reviews* 26, 579–584.
- Mayr, C., Lücke, A., Maidana, N., Wille, M., Haberzettl, T., Corbella, H., Ohlendorf, C., Schäbitz, F., Fey, M., Janssen, S., Zolitschka, B., 2009. Isotopic fingerprints on lacustrine organic matter from Laguna Potrok Aike (southern Patagonia, Argentina) reflect environmental changes during the last 16,000 years. *Journal of Paleolimnology* 42, 81–102.
- Mazaud, A., Kissel, C., Laj, C., Sicre, M.A., Michel, E., Turon, J.L., 2007. Variations of the ACC-CDW during MIS3 traced by magnetic grain deposition in midlatitude South Indian Ocean cores: connections with the northern hemisphere and with central Antarctica. *Geochemistry Geophysics Geosystems* 8, doi:10.1029/2006GC001532.
- Mazzarini, F., D’Orazio, M., 2003. Spatial distribution of cones and satellite-detected lineaments in the Pali Aike Volcanic Field (southernmost Patagonia): insights into the tectonic setting of a Neogene rift system. *Journal of Volcanology & Geothermal Research* 125, 291–305.
- McCormac, F., Hogg, A., Blackwell, P., Buck, C., Higham, T., Reimer, P., 2004. SHCal104 Southern Hemisphere Calibration 0–11,000 cal kyr BP. *Radiocarbon* 46, 1087–1092.
- McCulloch, R.D., Fogwill, C.J., Sugden, D.E., Bentley, M.J., Kubik, P.W., 2005. Chronology of the Last Glaciation in central strait of Magellan and Bahía Inútil, Southernmost South America. *Geografiska Annaler, Series A: Physical Geography* 87, 289–312.
- Naranjo, J.A., Stern, C.R., 1998. Holocene explosive activity of Hudson Volcano, southern Andes. *Bulletin of Volcanology* 59, 291–306.
- Petit, J.R., Jouzel, J., Raynaud, D., Barkov, N.I., Barnola, J.M., Basile, I., Bender, M., Chappellaz, J., Davis, M., Delaygue, G., Delmotte, M., Kotlyakov, V.M., Legrand, M., Lipenkov, V.Y., Lorius, C., Pepin, L., Ritz, C., Saltzman, E., Stievenard, M., 1999. Climate and atmospheric history of the past 420,000 years from the Vostok ice core, Antarctica. *Nature* 399, 429–436.
- Pugh, R.S., McCave, I.N., Hillenbrand, C.D., Kuhn, G., 2009. Circum-Antarctic age modelling of Quaternary marine cores under the Antarctic circumpolar current: ice-core dust-magnetic correlation. *Earth and Planetary Science Letters* 284, 113–123.
- Rabassa, J., Clapperton, C.M., 1990. Quaternary glaciations of the southern Andes. *Quaternary Science Reviews* 9, 153–174.
- Reimer, P.J., Baillie, M.G.L., Bard, E., Bayliss, A., Beck, J.W., Bertrand, C.J.H., Blackwell, P.G., Buck, C.E., Burr, G.S., Cutler, K.B., Damon, P.E., Edwards, R.L., Fairbanks, R.G., Friedrich, M., Guilderson, T.P., Hogg, A.G., Hughen, K.A., Kromer, B., McCormac, G., Manning, S., Ramsey, C.B., Reimer, R.W., Remmele, S., Southon, J.R., Stuiver, M., Talamo, S., Taylor, F.W., van der Plicht, J., Weyhenmeyer, C.E., 2004. IntCal04 terrestrial radiocarbon age calibration, 0–26 Cal Kyr BP. *Radiocarbon* 46, 1029–1058.
- Richter, T., Van der Gaast, S., Koster, B., Vaars, A., Gieles, R., De Stijter, H., De Haas, H., Van Weering, T., 2006. The Avaatech XRF core scanner: technical description and applications to NE Atlantic sediments. In: Rothwell, R.G. (Ed.), *New Techniques in Sediment Core analysis*. Geological Society, London, Special Publications, pp. 39–50.
- Roig, F.A., Le-Quesne, C., Boninsegna, J.A., Briffa, K.R., Lara, A., Grudd, H., Jones, P.D., Villagran, C., 2001. Climate variability 50,000 years ago in mid-latitude Chile as reconstructed from tree rings. *Nature* 410, 567–570.
- Röthlisberger, R., 2005. IGBP PAGES/World Data Center for Paleoclimatology. EPICA Dome C Ice Core nss-Ca and Na Data. [ftp://ftp.ncdc.noaa.gov/pub/data/paleo/icecore/antarctica/epica\\_domec/edc-ca-na.txt](ftp://ftp.ncdc.noaa.gov/pub/data/paleo/icecore/antarctica/epica_domec/edc-ca-na.txt) (accessed 21.12.07).
- Röthlisberger, R., Bigler, M., Wolff, E.W., Joos, F., Monnin, E., Hutterli, M.A., 2004. Ice core evidence for the extent of past atmospheric CO<sub>2</sub> change due to iron fertilisation. *Geophysical Research Letters* 31, L16207. doi:10.1029/2004GL020338.
- Röthlisberger, R., Mulvaney, R., Wolff, E.W., Hutterli, M.A., Bigler, M., Sommer, S., Jouzel, J., 2002. Dust and sea salt variability in central East Antarctica (Dome C) over the last 45 kyr and its implications for southern high-latitude climate. *Geophysical Research Letters* 29, doi:10.1029/2002GL015186.
- Skewes, M.A., 1978. Geología, petrología, quimismo y origen de los volcanes del área de Pali-Aike, Magallanes, Chile. *Anales del Instituto de la Patagonia* 9, 95–106.
- St-Onge, G., Mulder, T., Francus, P., Long, B., 2007. Chapter two. Continuous physical properties of cored marine sediments. In: Hillaire-Marcel, C., De Vernal, A. (Eds.), *Developments in Marine Geology*. Elsevier, pp. 63–98.
- Stern, C.R., 1990. Tephrochronology of southernmost Patagonia. *National Geographic Research* 6, 110–126.
- Stine, S., 1998. Medieval climatic anomaly in the Americas. In: Issar, A.S., Brown, N. (Eds.), *Water, Environment and Society in Times of Climatic change*. Kluwer Academic Publishers, Dordrecht, pp. 43–67.
- Stuiver, M., Reimer, P., 1993. Extended 14C database and revised CALIB radiocarbon calibration program. *Radiocarbon* 35, 215–230.

- Sugden, D.E., McCulloch, R.D., Bory, A.J.-M., Hein, A.S., 2009. Influence of Patagonian glaciers on Antarctic dust deposition during the last glacial period. *Nature Geoscience* 2, 281–285.
- Tucker, M.E., 1991. *Sedimentary petrology: an introduction to the origin of sedimentary rocks*. Blackwell Science Publications, Cambridge.
- Unkel, I., Björck, S., Wohlfarth, B., 2008. Deglacial environmental changes on Isla de los Estados (54.4°S), southeastern Tierra del Fuego. *Quaternary Science Reviews* 27, 1541–1554.
- Villa-Martínez, R., Moreno, P.I., 2007. Pollen evidence for variations in the southern margin of the westerly winds in SW Patagonia over the last 12,600 years. *Quaternary Research* 68, 400–409.
- Weninger, B., Jöris, O., Danzeglocke, U., 2004. Calpal - the Cologne radiocarbon CALibration and PALaeoclimate research package. <http://www.calpal.de>.
- Whitlock, C., Moreno, P.I., Bartlein, P., 2007. Climatic controls of Holocene fire patterns in southern South America. *Quaternary Research* 68, 28–36.
- Wille, M., Maidana, N.I., Schäbitz, F., Fey, M., Haberzettl, T., Janssen, S., Lücke, A., Mayr, C., Ohlendorf, C., Schleser, G.H., Zolitschka, B., 2007. Vegetation and climate dynamics in southern South America: the microfossil record of Laguna Potrok Aike, Santa Cruz, Argentina. *Review of Palaeobotany and Palynology* 146, 234–246.
- Wintle, A.G., 1973. Anomalous fading of thermoluminescence in mineral samples. *Nature* 245, 143–144.
- Yung, Y.L., Lee, T., Wang, C.-H., Shieh, Y.-T., 1996. Dust: a diagnostic of the hydrologic cycle during the last glacial maximum. *Science* 271, 962–963.
- Zolitschka, B., Mingram, J., Van der Gaast, S., Jansen, J.H.F., Naumann, R., 2001. Sediment logging techniques. In: Last, W.M., Smol, J.P. (Eds.), *Tracking Environmental Change Using Lake Sediments. Basin Analysis, Coring, and Chronological Techniques*, vol. 1. Kluwer Academic Press, Dordrecht, pp. 137–153.
- Zolitschka, B., Schäbitz, F., Lücke, A., Corbella, H., Ercolano, B., Fey, M., Haberzettl, T., Janssen, S., Maidana, N., Mayr, C., Ohlendorf, C., Oliva, G., Paez, M.M., Schleser, G.H., Soto, J., Tiberi, P., Wille, M., 2006. Crater lakes of the Pali Aike Volcanic Field as key sites for paleoclimatic and paleoecological reconstructions in southern Patagonia, Argentina. *Journal of South American Earth Sciences* 21, 294–309.